

Chapter – 3

*Experimental Techniques: γ -Ray Spectroscopy with
Multi Clover Detectors*

3.1. Introduction

The development of in-beam γ -ray spectroscopy took place in close relation with the development of detection techniques. The introduction of germanium detectors in the late sixties increased the resolution performances by several factors. This gave a significant advancement in the study of nuclear structure leading towards the discovery of the backbending phenomenon [1, 2]. The construction of arrays of composite Ge detectors along with BGO (bismuth germanate) escape-suppression shields detectors in the eighties gave an improvement of the peak-to-total ratio by a factor of ≈ 4 . The use of arrays of anti-Compton spectrometers made possible the discovery of superdeformed bands in medium-heavy nuclei at high spins [3]. The later technological advances, with the construction of the large arrays EUROBALL in Europe and GAMMASPHERE in the USA, INGA (Indian National Gamma Array) in India, AFRODITE (African Omnipurpose Detector for Innovative Techniques and Experiments) in South Africa, allowed for a detailed investigation of the exotic nuclear structure e.g., superdeformation, magnetic rotation etc. This chapter will present the main features of the interaction of γ -rays and detector arrays.

3.2. Interaction of γ -Rays with Matter

Excited states in a nucleus tend to be unstable and hence decay to the ground state. The excited states can decay in more than one way, but the most common is by the emission of a γ -ray. The characteristics of the γ -ray depend on those of the initial and final states that it links and hence, by the observation of rays, information on the excited states of the nucleus can be inferred. The energy of the emitted γ -ray is governed by the laws of energy conservation and is therefore equal to the difference between the energies of the initial and final states, minus a recoil correction which is normally negligible [4].

Detection of γ -rays is possible as a result of their interaction with the detector material. Although a large number of possible interaction mechanisms are known for γ -rays in matter, only three major types of interactions play an important role in radiation measurements: *photoelectric absorption, Compton scattering, and pair production*. All these processes lead to the partial or complete transfer of the γ -ray photon energy to electron energy. They result in sudden and abrupt changes in γ -ray photon history, in that photon either disappears entirely or is scattered through a significant angle.

3.2.1. Photoelectric Absorption

In the photoelectric absorption process, a photon undergoes an interaction with an absorber atom in which the photon completely disappears. In its place, a photoelectron is produced from one of the electron shells of the absorber atom with a kinetic energy given by the incident photon energy ($h\nu$) minus the binding energy of the electron in its original shell (E_b). This process is shown in the Fig. 3.1 below. For typical γ -ray energies, the photoelectron is most likely to emerge from the K shell, for which typical binding energy range from a few keV for low-Z materials to tens of keV for materials with higher atomic number. The photoelectrons appears with an energy given by

$$E_{e^-} = h\nu - E_b, \quad (3.1)$$

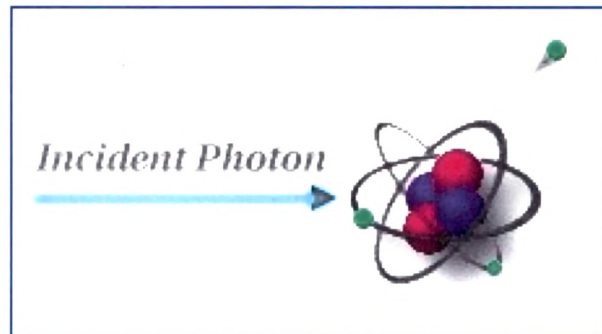


Figure 3.1: Photoelectric absorption.

The vacancy that is created in the electron shell as a result of the photoelectron emission is quickly filled by electron rearrangement. In the process, the binding energy is liberated in the form of a characteristic X-ray. Thus, the effect of photoelectric absorption is the liberation of a photoelectron, which carries off most of the γ -ray energy, together with one or more low-energy electrons corresponding to absorption of the original binding energy of the photoelectron. The total electron kinetic energy equals the incident γ -ray energy and will always be the same if mono-energetic γ -rays are involved. The differential distribution of the electron kinetic energy for a series of photoelectric absorption events would be a simple delta function as shown in Fig. 3.2. The single peak appears at a total electron energy corresponding to the energy of the incident γ -rays.

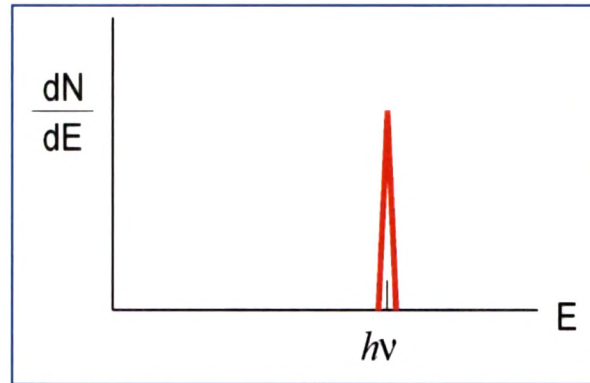


Figure 3.2: The photoelectric absorption in differential pulse height γ -ray spectrum.

3.2.2. Compton Scattering

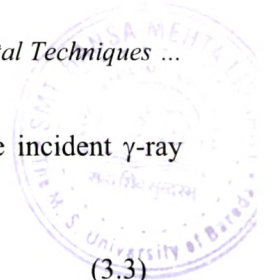
The interaction process of a Compton scattering process takes place between the incident γ -ray photon and an electron in the absorbing material. It is most often the predominant interaction mechanism for γ -ray energies.

In Compton scattering, the incoming γ -ray photon is deflected through an angle θ with respect to its original direction. The photon transfers a portion of its energy to the electron (at rest), which is then known as a recoil electron. The scattering angle θ is dependent upon the fraction of the photon energy that is transferred to the electron. An illustration of the Compton scattering process is given in the Fig. 3.3.

The expression that relates the energy transfer and the scattering angle is given as,

$$h\nu' = \frac{h\nu}{1 + \frac{h\nu}{m_0c^2}(1 - \cos\theta)}, \quad (3.2)$$

where, m_0c^2 is the rest mass energy of the electron. For small scattering angles θ , very little energy is transferred. From the above equation it is seen that the maximum energy transfer to the electron occurs when the γ -ray is back scattered ($\theta = 180^\circ$), but even at this value, the recoil electron energy is less than E_γ . "This is referred to as *Compton Edge*". Some of the original energy is always retained by the incident photon, even in the extreme of $\theta = \pi$. Hence, the Compton scattering never results in a complete energy deposition, but will lead to an undesirable continuous background at energies lower than the incident γ -ray energy; referred to as *Compton background*. For any one γ -ray energy, the electron energy distribution has the general shape shown in the Fig. 3.4.



The gap between the maximum Compton recoil electron and the incident γ -ray energy is given by

$$E_C \equiv h\nu - E_e - |\theta=\pi| = \frac{h\nu}{1+2h\nu/m_0c^2}, \tag{3.3}$$

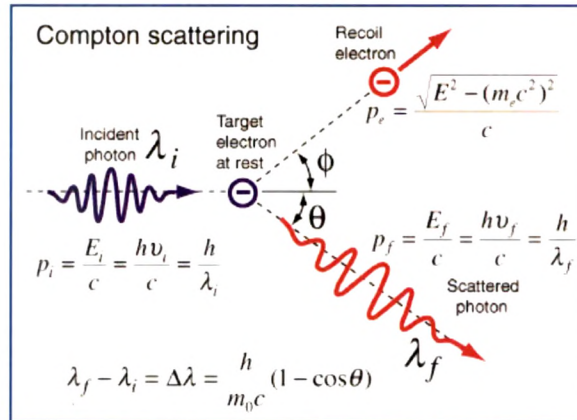


Figure 3.3: Compton Scattering.

In the limit that the incident γ -ray energy is large, or $h\nu \gg m_0c^2/2$, this energy difference tends towards a constant value given by

$$E_C \cong \frac{m_0c^2}{2} (= 0.256MeV) \tag{3.4}$$

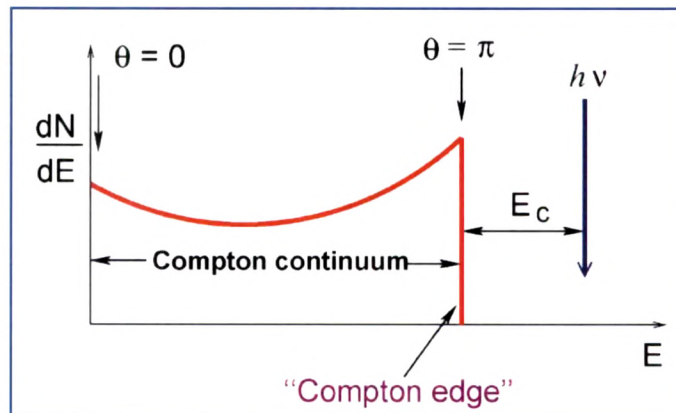


Figure 3.4: Compton scattering process in pulse height γ -ray spectrum.

3.2.3. Pair Production

The third type of interaction is pair production, as shown in Fig. 3.5. If a γ -ray has an energy exceeding twice that of the electron rest-mass energy (1.02 MeV), the process of pair production is energetically possible. The interaction must take place in the Coulomb field of a nucleus, and the γ -ray photon disappears and is replaced by an electron-positron pair. All the excess energy carried in by the photon above the 1.02 MeV thresholds goes into kinetic energy shared by the electron and the positron. The probability of this interaction occurring remains very low until the γ -ray energy approaches several MeV, so therefore the pair production process is confined to only high-energy γ rays.

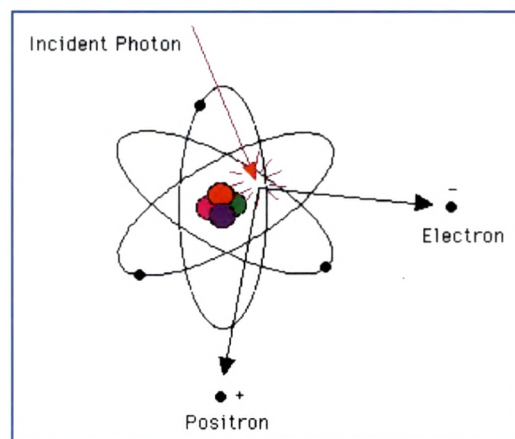


Figure 3.5: Pair Production.

The electron and positron created will only travel a few millimetres before losing all of their kinetic energy to the absorbing material. The positron will annihilate with a normal electron in the absorbing medium, creating two annihilation photons, each with energy of 511-keV. These photons can then either interact with the absorbing medium, or escape the detector. If both annihilation photons are stopped in the detector, then a photopeak corresponding to the energy of the original γ -ray is seen. If the annihilation photons both escape the detector, the total charged-particle kinetic energy created by the incident ray is a clean peak, as in the photoelectric effect, but located $2m_e c^2$ below the incident γ -ray energy, where m_e is the rest mass energy of the electron. This is known as the double-escape peak. Another common scenario is that one of the annihilation photons is completely absorbed by the detector but the second photon escapes. This result in a peak located $m_e c^2$ below the incident γ -ray energy and is known as the single-escape

peak. This is shown in Fig. 3.6. There is no simple expression for the probability of pair production per nucleus, but the magnitude varies approximately as Z^2 of the absorbing material. All interaction processes increase with atomic number Z , hence it is useful that the γ -ray detectors incorporate elements with a high atomic number. The two most common forms of this are semiconductor and scintillation detectors.

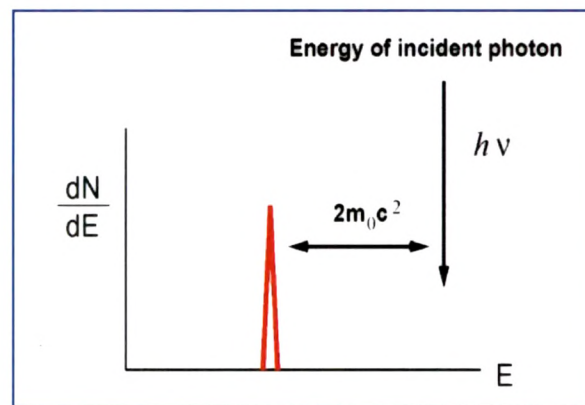


Figure 3.6: Pair production process in pulse height γ -ray spectrum.

3.3. Detection of γ -Rays

When a nucleus de-excites, it emits radiation in the form of γ -rays, containing the information on the structure of the nucleus. It is of paramount importance that the γ -ray detector used should have excellent energy resolution with a substantial detection efficiency along with good timing response. Semiconductor detectors are preferably used to detect γ photons since they fill these criteria. The incident γ -ray photon produces electron-hole pairs which can be collected by applying a voltage across the detector material. A semiconductor with a lower band-gap and a low level of impurities is preferred. A material with a higher atomic number is also preferred for detectors as it provides a high absorption coefficient for the incident γ radiation. From these considerations, silicon and germanium are the two ideal candidates. Germanium detectors, due to their inherent excellent energy resolution find extensive application in the γ -ray spectroscopy. The germanium detector is essentially a reverse biased p - n junction. At the junction between the p -type and n -type material, the migration of electrons from the n -type material and holes from the p -type material results in the formation of a region of net zero charge. This region is known as the *depletion region*, a

region devoid of any mobile charge carriers. An electric field gradient is set-up across the depletion region, due to the presence of the positive charge on the n-side of the junction, and the negative charge on the p-side. γ -rays interacting with the germanium will produce electron-hole pairs. It is desirable that the interaction occurs within the depletion region so that a one-to-one correspondence between the created electron-hole pairs and the incident γ radiation is maintained. In normal semiconductor detectors, the depletion region is ≈ 3 mm thick. The thickness (d) of the depletion region is given by,

$$d = \sqrt{\frac{2\varepsilon V}{eN}}, \quad (3.5)$$

where, V is the applied reverse bias voltage, N is the net impurity concentration, ε is the dielectric constant and e is the electronic charge. From the equation it is evident that a decrease in the net impurity content will result in a corresponding increase in the size of the depletion region. Pure germanium can only sustain a depletion depth of about a few millimetres before electrical breakdown occurs. Advances in manufacturing techniques have, now allowed extremely pure Ge crystals to be grown. High purity germanium (HPGe) detectors have an impurity levels as low as 10^9 atoms/cm³, compared to the 10^{12} atoms/cm³ for normal semiconductors. With such low impurity concentration depths of about several centimetres could be achieved.

Now a γ -ray interacting with the HPGe crystal will create a number of free electron-hole pairs. The number of free electron-hole pairs thus generated within the depletion region of the crystal depends on the energy of the incident γ -ray. To eliminate other excitations by thermal energy, the detector is operated at liquid nitrogen temperatures (77° K). A high voltage is usually applied across the detector crystal so that the generated free electron-hole pairs will be drifted by the electric fields towards the electrode and then be collected at the electrode. These electrons will flow through an electric circuit and an electrical signal is available.

3.4. Fundamental Properties of γ Detector Arrays

The features of a γ -detector array can be defined by three main parameters: the energy resolution ΔE_γ , the total photopeak efficiency P_{ph} and the peak-to-total ratio P/T . Ultimately, these three parameters will determine the figure of merit of the γ -detector arrays, which is the *observational limit*, defined as the minimum intensity of a γ -ray

transition that can be detected. The performance of a γ detector array depends on the intrinsic parameters of the array, on the detectors composing the array, as well as on the existing experimental conditions. Among the experimental conditions, the multiplicity of the γ -rays will influence the photopeak efficiency and peak-to-total ratio, whereas the velocity of the recoils produced in heavy-ion reactions will cause a Doppler shift of the γ -ray lines, influencing the energy resolution. Nevertheless, if the angle of the γ -ray emission is known, correction for the Doppler shift can be made.

In the following, the fundamental parameters characterizing a γ -detector array will be defined.

3.4.1. Energy Resolution

The total energy resolution of the detector array is determined by the intrinsic resolution of the individual detectors $\Delta E_{\gamma}^{(intr.)}$, and by the energy spread due to the Doppler effects which takes place for in-beam experiments $\Delta E_{\gamma}^{(Doppler)}$:

$$\Delta E_{\gamma} = \sqrt{(\Delta E_{\gamma}^{(intr.)})^2 + (\Delta E_{\gamma}^{(Doppler)})^2}, \quad (3.6)$$

The typical energy resolution of a Ge detector is $\Delta E_{\gamma} = 2\text{-keV}$ for an energy of $E_{\gamma} = 1.33\text{ MeV}$. One should note that if segmented Ge detectors are used, and the total energy E_{γ} is calculated as a sum of the energies deposited in the various segments $E_{\gamma}^{(i)}$, the resolution is calculated:

$$\Delta E_{\gamma}^{(intr.)}(E_{\gamma}) = \sqrt{\sum_{i=1}^{N_S} \Delta E_{\gamma}^{(i)}(E_{\gamma}^{(i)})}, \quad (3.7)$$

where, N_S is the number of segments which fire.

The Doppler effects depend on the existing experimental conditions although it can be reduced by having known more precisely the angle at which the γ -ray is emitted. In principle, three factors contribute to the Doppler broadening. (1) the finite solid angle within which the incident γ -ray interaction is detected; (2) the angular spread of the recoiling nuclei and (3) the variation of the recoils due to the slowing down in the target. The γ -ray emitted by a recoiling nucleus has energy,

$$E_{\gamma} = E_{\gamma}^0(1 + \beta \cos \theta), \quad (3.8)$$

To the first order, where E_γ^0 , is the 'true' γ -ray energy or the energy of a photon emitted if the nucleus was not moving, $\beta = v/c$, the recoil velocity of the nucleus, and θ is the angle between the detector and the recoil axis of the nucleus. A relation which gives the connection between the angle of emission θ_γ , the half-operating angle of detection $\Delta\theta_\gamma$ and the Doppler broadening $\Delta E_\gamma^{(Doppler)}/E_\gamma$ is:

$$\frac{\Delta E_\gamma^{(Doppler)}}{E_\gamma} = 2 \frac{v_r}{c} \sin \theta_\gamma \sin \Delta\theta_\gamma, \quad (3.9)$$

where, v_r is the recoil velocity.

If the directions of the recoils have an angular spread, the precision of the angle θ_γ will be further limited. Moreover, the relative variation of the recoil velocity which is typically $\Delta v_r/v_r \approx 0.1$ will also limit the attainable energy resolution. Nevertheless, the last two factors can be minimized by measuring the recoil angle with position sensitive recoil detectors and by determining the recoil velocity v_r by using time - of - flight techniques.

3.4.2. Photopeak Efficiency and Peak-to-Total Ratio

The absolute efficiency of a γ -ray detector system ϵ_{abs} is defined as the number of events recorded divided by the total number of quanta emitted by the source. In a detector array, this absolute efficiency is related to the intrinsic efficiency ϵ_{int} of the individual detectors by:

$$\epsilon_{abs} = \frac{N\Omega}{4\pi} \epsilon_{int}, \quad (3.10)$$

where, N is the number of detectors and Ω is the solid angle covered by an individual detector when viewed from the source. The intrinsic detector efficiency is defined as the ratio of the number of recorded events to the number of quanta incident on detector. In general, ϵ_{int} depends on the detector material, its geometry (thickness) and energy of the incident γ -ray. Since the detection of γ -rays which deposit their whole energy are of interest, the important parameter which represents the detection efficiency is the photopeak efficiency ϵ_{ph} . The value of the photopeak efficiency ϵ_{ph} is proportional to the absolute efficiency ϵ_{abs} , with a proportionality factor given by the peak-to-total ratio P/T :

$$\epsilon_{ph} = \frac{P}{T} \epsilon_{abs}, \quad (3.11)$$

The peak-to-total ratio (P/T) for a γ -ray of energy E_γ is the ratio between the number of photopeak events and the total number of detected events, which include the photopeak and Compton background. Both *photopeak efficiency* and *peak-to-total ratio* depend on the energies of the γ rays, but are affected by the multiplicity of the γ -ray event as well. The peak-to-total ratio $(P/T)_{M_\gamma}$ for γ -rays of multiplicity M_γ can be approximated by the relation:

$$\left(\frac{P}{T}\right)_{M_\gamma} = W(M_\gamma) \left(\frac{P}{T}\right), \quad (3.12)$$

Where (P/T) corresponds to a multiplicity $M_\gamma = 1$ and $W(M)$ is the probability of having non-overlapping interactions from different incident γ -rays of multiplicity M_γ (the isolated hit probability).

3.4.3. Observational Limit

For an objective comparison of the sensitivities of various γ -ray detector arrays, the observational limit was introduced as the *figure-of-merit* of γ -detector arrays for high multiplicity events. The *observational limit* is defined as the minimum intensity of a γ -ray transition which can be observed. The *observational limit* is determined by the minimum number of counts a γ -ray peak has to have on a fluctuating background to be statistically significant. A typical nuclear spectroscopy experiment involves a cascade of M_γ transitions occurring in the de-excitation of a highly excited nucleus. Usually, the number of detected events (called fold) F is less than the multiplicity M_γ . In this context, it is of interest to determine the number of counts $N_p^{(F)}$ detected in an F -dimensional peak, given the intensity I_0 of the cascade involving M_γ transitions. This can be estimated from

$$N_p^{(F)} = \left(0.76 \frac{P}{T}\right)^F \frac{I_0 N_c^{(F)} F!}{M!}, \quad (3.13)$$

The factor 0.76 results from the consideration of a F -dimensional volume element determined by the FWHM of the γ -ray peak. The value $N_c^{(F)}$ represents the number of F -fold coincidences obtained by combining the measured F' -fold coincidences with $F \leq F' \leq M$ as:

$$N_c^{(F)} = \sum_{F'=F}^M N(F') \frac{F!}{F!(F'-F)!} \quad (3.14)$$

The distribution in the number of F' -fold coincidences $N(F')$ depends mainly on the multiplicity M , and the array photopeak efficiency ϵ_{ph} . The intensity I_0 is a relative value, being normalized to the sum of intensities of all cascades which feed the ground state.

3.4.4. Detection Efficiency

The detection efficiency corresponds to the probability of detecting a photon in the detector. The following efficiencies can be defined:

- The Absolute Efficiency

$$E_{abs} = \frac{N_{det}}{\Omega N_{emitted}}, \quad (3.15)$$

where, N_{det} is the number of events detected, Ω is the solid angle covered by the detector, and $N_{emitted}$ is the number of γ -rays emitted by the source.

- The Photopeak Efficiency

$$E_{ph} = \frac{N_{peak}}{\Omega N_{emitted}}, \quad (3.16)$$

where, N_{peak} is the number of γ -rays in the photpeak.

- The Relative Efficiency

$$E_{rel} = \frac{(E_{ph}\Omega)_{detector}}{(E_{ph}\Omega)'_{NaI}}, \quad (3.17)$$

where, $(E_{ph}\Omega)'_{NaI} = 1.244 \times 10^{-3}$ for a NaI detector of 7.6 cm length and 7.6 cm diameter at a distance of 25cm from the source.

3.4.5. Escape Suppression

A major improvement in the peak to total ratio of a Ge detector can be made if the events where a γ -ray scatters out of the crystal and so has not deposited the full photopeak energy can be rejected. To achieve this, the Ge crystal can be surrounded by a shield comprised of scintillator detectors. This shield acts as a veto signal for the Ge detector by rejecting the unwanted events. A good shield will be made of high efficiency scintillator since the resolution is not important, the usual scintillator used for γ -ray spectroscopy being bismuth germinate (BGO).

3.4.6. Compton Suppression

The energy required to create an electron-hole pair in germanium is approximately 2.96 eV. Thus, an incident γ -ray, with an energy of several hundred keV, produces a large number of such pairs, which results in a superior energy resolution as compared to other detectors (the energy required to create an information carrier in gas detector is approximately 30 eV, whereas in scintillator it is approximately 2 to 500 eV). The energy resolution of a detector is directly proportional to the number of information carriers created by the incident radiation. The γ -ray resolution of HPGGe detector is typically of the order of 2-keV at 1 MeV. For a 1 MeV γ -ray, Compton scattering contributed significantly to the interaction process. The Compton scatters events results in a continuum background. For a 125 cm³ Ge crystal, a 1 MeV γ -ray has an absorption probability of about 75%. This implies that about 25% of the incident γ -rays do not correspond to the full energy (photo-peak) information while the rest 80% contribute to the undesired Compton background. For a mono energetic γ -ray, we define a quantity P, termed as Peak-to-Total, as

$$P = \frac{\text{number of counts in the photopeak}}{\text{total number of counts in the background}} \quad (3.18)$$

The measurements for the suppressed and unsuppressed spectra were taken with a ⁶⁰Co source and the resulted spectrum is shown in Fig. 3.7. At $E_\gamma = 1$ MeV, a typical detector (with efficiency $\eta = 23\%$), would have a peak-to-total to about 20%. Thus, about 80-85% events in the Ge detector do not correspond to the desired (useful) energy information, but only contribute towards the background, which submerges the weak γ -rays. Now if we were to consider the coincidence scenario, where two γ -rays are in coincidence (γ - γ coincidence), out of the 15-20% of the events wherein a photpeak event has been recorded by the individual detectors, only 2-4% of the recorded events contain no useful information, yet they contribute substantially to the background which mask the weak yet interesting γ -rays. However, the situation can be improved drastically by using Compton suppression shields (also referred as escape suppression shields).

In order to reduce the contribution of scattered γ -rays (Compton scattered), the Ge detector can be surrounded by an inorganic scintillator detector. The scintillator shield is used to detect the photons that are Compton scattered from the Ge crystal. The shield is operated in *anti-coincidence* with the Ge detector, in order to electronically veto out events associated with Compton scattering from the Ge crystal. This is illustrated in Fig.

3.8. The collimator ensures that the anti-Compton shield does not view the source of γ -radiation directly but detects only the γ -transitions that are Compton scattered from the HPGe and hence the shield does not record a event in coincidence with the HPGe detector. However, since γ_2 interact with the detector via Compton scattering, the emitted secondary photon is recorded by the shield. Hence, both the HPGe and shield record events, in coincidence. Such events then correspond to partial energy deposition in the HPGe and have to be electronically vetoed.

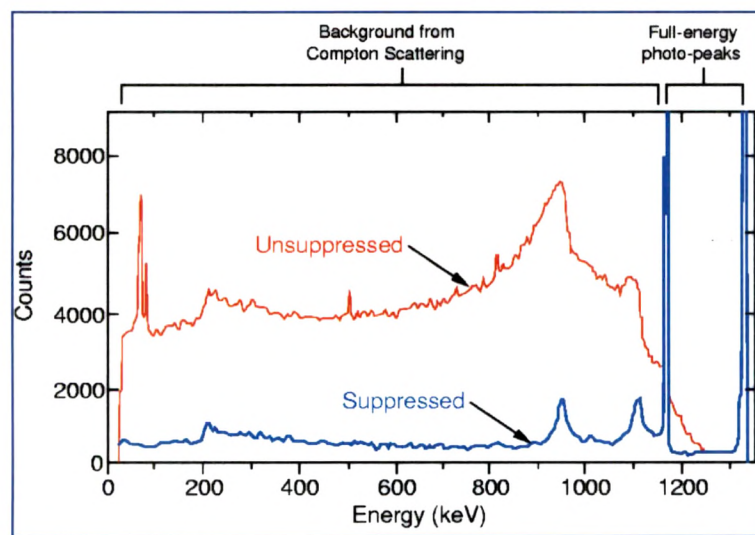


Figure 3.7: Shows the suppressed and unsuppressed spectra from the ^{60}Co source.

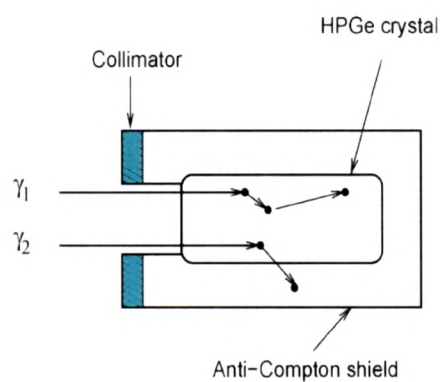


Figure 3.8: Working principle of Compton suppression.

Thus, the majority of the events recorded using such a coupled system (Ge + scintillator shield) correspond to the events which have resulted in a full energy

deposition in the HPGe (*i.e.*, events originating from photopeak interactions). The low Compton background obtained with this system enhances the peak-to-total value up to about 50 - 60%, at energy of 1 MeV. Modern day Compton shields are made of Bismuth Germanate Oxide (BGO, $\text{Bi}_4\text{Ge}_3\text{O}_{12}$). It has a higher density (7.13 gm/cm^3) and hence a large attenuation co-efficient compared to NaI(Tl). Thus compact anti-Compton shield (ACS) could be fabricated using BGO. A multi-detector array using such Compton suppressed detectors would then accommodate a large number of such detector units, which results in an enhanced detection limit of the array.

3.5. γ -Ray Detectors

Composite Detector

The advancement in experimental nuclear spectroscopy has been possible due to the development in the detector fabrication techniques which has made available efficient detectors. The size of the detector plays an important role as a larger size increases the detection solid angle and hence its detection efficiency. The limitation of using a large single crystal arises from:

1. The large detection angle results in considerable Doppler broadening of the observed γ -rays, which deteriorates the inherent resolution.
2. The large time spread in the transit and collection time of the electron-hole pairs produced in the crystal results in very poor timing characteristics.
3. Large volume crystals are prone to neutron damage.

The photopeak efficiency of a detector can be increased by increasing the size of the Ge crystal. Crystals of size larger than 6 cm diameter are difficult to fabricate. In addition, they have poor charge collection time and greater sensitivity to neutron damage. For in-beam spectroscopy, they suffer from increased Doppler broadening from γ -rays. An economical way of increasing detector volume is by accommodating more than one Ge crystal within the same cryostat surrounded by a common anti-Compton shield. Clovers detectors are one such detector, which contain four separate coaxial n-type germanium crystals [Fig. 3.9] packed together in a four leaf Clover arrangement. A common high voltage is applied to each crystal to the inner contacts and signals are obtained via AC - coupling.

3.5.1. Clover Detector

The Clover detector [5 - 9] comprises of four coaxial *n*-type HPGe crystals, 50mm in diameter and 70 mm in length mounted in a common cryostat arranged in a four-leaf Clover configuration. The typical dimensions of a Clover detector are shown in Fig. 3.10. and a Clover detector in Fig.3.11.

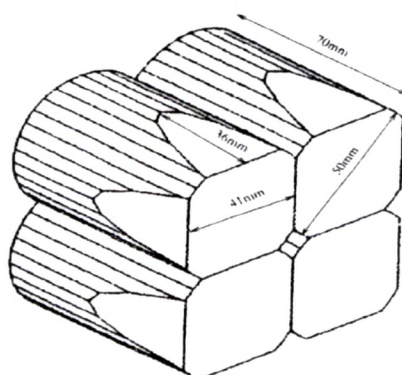


Figure 3.9: The segmented Clover germanium detector crystal and how are they packed inside the detector. A Clover detector consists of four *n* - type coaxial HPGe crystals.

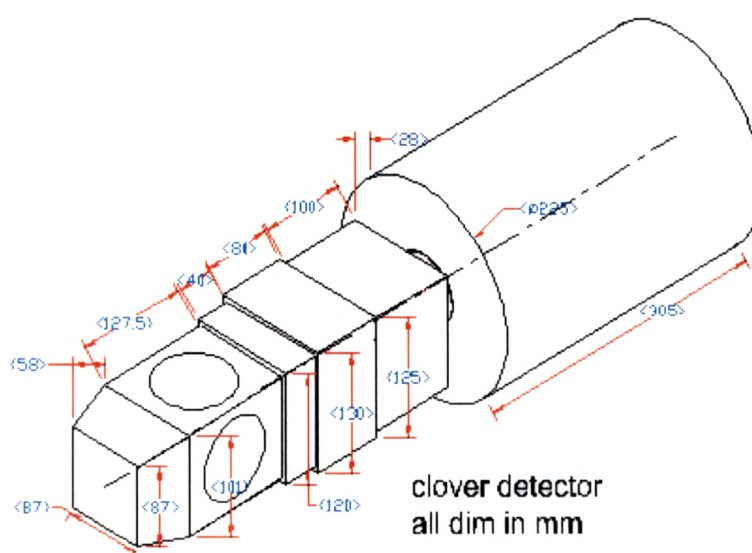


Figure 3.10: Dimensions of a typical Clover detector.

Each detector has a square front face with round edges obtained by tapering it on two adjacent faces. This enables a close packing of detectors with Ge - Ge distance of

about 0.2 mm with a total active volume of $\sim 470 \text{ cm}^3$, which is 89% of the original Ge volume. Each of the four crystals is an individual detector with independent outputs. A common ground (high voltage) is applied on the other (inner) contacts of the diodes. Each crystal element has its own preamplifier, which allows energies deposited in more than one element of a detector due to Compton scattering, to be added. This *add-back* procedure has been shown to significantly enhance Clover photopeak efficiency, particularly in the high energy regime ($E_\gamma \geq 1000\text{-keV}$). By including the scattered events, the relative efficiency for the Clover detector is on average 140%, comparing to the relative efficiency of $\sim 80\%$ for the large single-crystal Ge detectors [6].

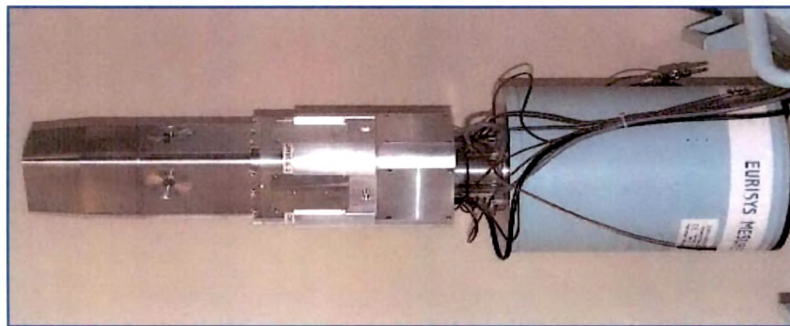


Figure 3.11: A Clover detector.

The energy signal is collected from each individual crystal from the inner contact via AC - coupling. The detection efficiency that can be obtained with the Clover detector is greater than the efficiency of the four separate single crystal detectors with the same volume. This is due to the ability of being able to treat the crystals separately and to *add-back* the Compton scattered events that occur between two or more crystals, resulting in the recovery of the photopeak energy. The small opening angles of the individual crystals also ensure that the observed γ transitions are not Doppler broadened. Although the individual relative efficiency of each crystal is only 23% (at $\sim 1 \text{ MeV}$ photon energy), the relative efficiency for the Clover detector is on average 140%. Composite detectors have several further advantages over single crystals. The intrinsic Clover geometry makes it suitable for use in *add-back* mode as a Compton polarimeter [6, 7, 10] to measure the linear polarization of γ -rays. This allows the magnetic or electric character of transitions to be determined from which it is often possible to deduce the parities of nuclear states. The polarization sensitivity of a Clover detector is reported in [10].

3.5.1.1. Add-Back Mode of a Clover Detector

As discussed in the previous section, the total photopeak efficiency of a Clover detector is the sum of two complementary effects: the full energy γ -ray absorption in each of the individual crystals and partial γ -ray absorption in two or more crystals of the detector. The four crystals are treated as individual detectors, it is expected that a Compton scattering will result in a data being recorded by two (or more) adjacent crystals. Since the data is recorded in an event-by-event mode, if two crystals of the same Clover have fired in a given event, in all probability the events in these crystals are due to Compton scattering and have resulted in a partial energy deposition in the individual crystals. The probability for two genetically related γ -rays (γ -rays in cascade) being detected by 3 crystals of the same Clover is extremely small due to small solid angle coverage by these individual crystals. If a single crystal Ge detector were to be used, the Compton scattered photon would be lost and we could have recorded only the partial energy in the single crystal. The process of recovering the partial energy deposited in the neighbouring crystals of the same Clover within the same event is referred to as *add-back* mode of operation.

The measurement for the photopeak efficiency, add-back factor and energy resolution of the Clover detector have been performed using the standard ^{152}Eu , ^{133}Ba and ^{207}Bi γ -ray calibration sources. The source was placed at a distance of about 23 cm from the detector. The data was recorded in the singles mode *i.e.*, when any one of the Clovers within the multi-Clover array had a non-zero data. This data set consisted of events where one, two, three or all four crystals within the same Clover had fired. The events where only one of the four crystals recorded a γ -ray, corresponds to a 1-fold event. If two of the four crystals recorded a γ -ray, then it is referred to as 2-fold event. It is unlikely that three (3-fold event) or all the four (4-fold event) crystals within the same Clover would record data originating from a single incident γ -ray. It is clear that the 1-fold events are due to photopeak absorption while all other folds correspond to Compton scattering. Since the events (for the same gamma transition) are added to recover the total photopeak energy, this mode results in a considerable enhancement in the efficiency of the Clover detector.

It was observed that the photopeak efficiency for a single crystal is lower than the efficiency in the add-back mode. For example, the efficiency of a Clover detector in the add-back mode is almost 6 times the average efficiency of each crystal especially at high energies (at $E_\gamma \sim 1000\text{-keV}$) where the contribution from the Compton scattering is

dominant. This substantial improvement in the efficiency of a Clover detector is depicted in Fig. 3.12. Hence the Clover detectors in the add-back mode substantially increases the detection efficiency especially at higher E_γ i.e. $E_\gamma \geq 1$ MeV, since the photopeak energy could be recorded from the individual partial energies recorded by the single crystals.

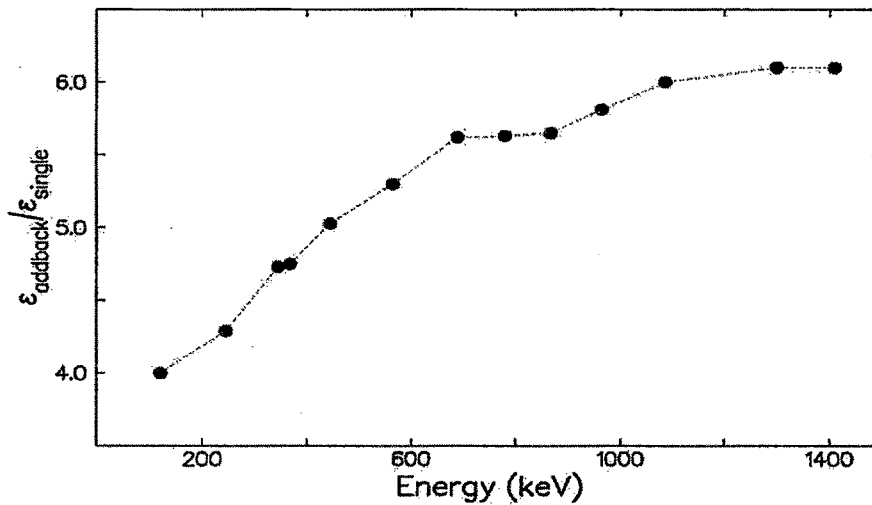


Figure 3.12: Ratio of the photopeak efficiency of the Clover detector in addback mode to the average efficiency of a single crystal.

3.5.2. LEPS Detector

LEPS: Low Energy Photon Spectrometers [11]

LEPS Detectors are planar made from a single crystal of p-type HPGe with the dimensions 10mm thick and 60mm in diameter. Each crystal is electrically segmented into four quadrants. The signal from each quadrant is processed separately, as in the case of Clovers. One consequence of the planar geometry is that LEPS efficiency falls off much faster with increasing energy than that of Clovers and that is negligible above ~ 400 MeV, since the low energy photons are likely to Compton scatter out of the crystal. LEPS are thus neither BGO suppressed nor operated with *add-back*. The LEPS detectors are more efficient in detecting the low energy ($\approx 30 - 300$ keV) γ -rays.

3.6. Detector Arrays for Nuclear Spectroscopy

The existing γ -ray detector arrays represent multi-detector arrangements of anti-Compton spectrometers, optimized for high energy resolution, high efficiency and high peak-to-

total ratio. The excellent energy resolution of the Ge detectors is degraded in in-beam spectroscopy experiments due to a Doppler broadening of the γ lines resulting from the fact that the nuclei are produced in nuclear reactions, flying usually with a velocity of $v/c \approx 4\%$, and due to the large solid angle of the Ge detectors. A better definition of the γ -ray emission angle than the one provided by the detector opening would allow for a reduction of the Doppler broadening. Since for γ -rays with energies of up to ≈ 4 MeV, the dominant interaction modes are the Compton scattering and photoelectric effect, the detection systems are required to allow for a reduction of the Compton background in order to obtain a higher peak-to-total value.

The conventional anti-Compton spectrometers are formed by Ge detectors shielded against each other by surrounding anti-Compton detectors. This arrangement can only suppress the Compton-scattered γ -rays. The composite Ge detectors used in detector arrays like EUROBALL, GAMMASPHERE, INGA, AFRODITE however, consist of clusters of Ge detectors in a tight geometry and are surrounded by common BGO anti-Compton shields. Using this arrangement, the Compton-scattered events can be reconstructed, and the full energy can be obtained by summing the energies deposited in adjacent crystals (the so-called *add-back* mode of operation). In this way the efficiency of a composite detector can be considerably increased [7]. Unfortunately, if several γ -rays will interact in the same cluster of detectors, a decrease in the P/T (Photopeak to Total) ratio will occur due to the false summing of the energies of the detectors. For a correct assignment of the γ -ray interactions in the detectors to a certain incident γ -quanta, a method to “track” the interaction sequence will have to be introduced.

3.7. Need for a Detector Array

The counting rate in a single HPGe detector can be calculated by the equation

$$N_s = N_r(\Omega/4\pi)M\eta, \quad (3.19)$$

where, N_r is the number of residual nuclei produced per second, $(\Omega/4\pi)$ the solid angle coverage by each detector, M the number of photons emitted per event and η the total γ -ray detection efficiency of the detector after Compton suppression.

The total counting rate of a single detector is not, in general, allowed to exceed 10,000 counts per second to avoid excessive pile up. After Compton suppression, this rate becomes $\sim 3,000$ per second. In γ -ray spectroscopy, coincidence data are always preferred

to be collected since the resolving power improves considerably with this technique [12]. Moreover, coincidence relation is one of the most important criteria in assigning a γ -ray transition. Also, it helps in cleaning up the spectrum considerably. The more is the number of coincidence fold, the better the cleaning is. But the main disadvantage in that is the count rate goes down drastically with increasing number of fold in coincidence. The rates may be increased by increasing N_r , which in turn can be done by increasing beam current or target thickness. But again this is constrained by the pile-up problem. The coincidence count rate can neither be increased much by increasing the solid angle of individual detector, since with this increase the Doppler broadening of γ -rays also increases and moreover, the unwanted summing effect if the γ -rays increases.

The increase in rate can only be achieved by using an array of Compton suppressed HPGe detectors without effecting the quality of the data. Therefore, the arrays with larger and larger number of γ -ray detectors have been built up over the past decades worldwide. A review of these detector arrays is presented in the Ref. [6]. Data with higher fold coincidences are also possible with reasonable count rate with this kind of arrays.

3.8. Instrumentation for Large γ -Arrays

The spectroscopy of discrete γ -rays produced in a nuclear reaction received a large boost in the 70's with the availability of heavy-ion accelerators and large volume high energy resolution Ge detectors. The primary advantage intrinsic Ge detectors have over other types of detectors are (i) excellent energy resolution (< 2 keV at 1 MeV) (ii) large detection volume of 100 cc or more (iii) moderate photopeak efficiency (20% higher) (iv) excellent resistance to neutron damage and high electron-hole mobility for reduced charge collection time. Due to its low band gap (~ 0.67 eV), Ge detectors have to be cooled to near LN₂ temperatures to minimize thermal noise.

The most probable mechanism for interaction of photons of \sim MeV energy with Ge is through Compton scattering. Part of the energy of the interaction is transferred to one or more electrons through photoelectric or Compton process. For the measurement of the energy transferred to the electrons, the detector is kept in reverse biased by the application of strong electric field (\sim kV/cm). The energetic electrons passing through the sensitive volume of the crystal can induce electron-hole pairs which would flow towards the positive and negative electrodes. This charge can be collected and converted to an

output by a charge-sensitive pre-amplifier. The number of electron-hole pairs created, and thus the size of the output voltage, is proportional to the electron energy.

For a typical crystal of 6 cm diameter and 6 cm length, the photopeak efficiency is 40% relative to a 3" x 3" NaI crystal and a peak to total (P/T) ratio of ~ 0.2. The small P/T ratio of Ge detectors implies that only 1/5 of the detected events have the correct energy information. For γ - γ coincidence measurement, only 4% of the events are useful for energy calibration. The sensitivity of the detector setup to identify weak channels is considerably degraded due to the presence of large Compton background. It is possible to surround the Ge detector by another high-efficiency detector to identify the Compton scattered events and electronically veto them out. The first Compton-suppressed detector developed by Nolan *et al.*, [13] used NaI as the active scintillator. Six such Compton-suppressed detectors were used for the study of high spin states. Electronic suppression of events detected in the Ge detector increased the P/T ratio from 0.2 (unsuppressed) to 0.6 (suppressed). The anti-Compton detectors were shielded from the direct photons coming from the target by heavy-metal collimators.

The relatively large attenuation length of NaI made the shields quite bulky preventing further increase of Ge detectors in the array. The next generation of shields have been made of BGO ($\text{Bi}_4\text{Ge}_3\text{O}_{12}$) crystals. To suppress the forward-scattered photons, the space behind the germanium detector is filled by another BGO element. (Refer Fig. 3.13)

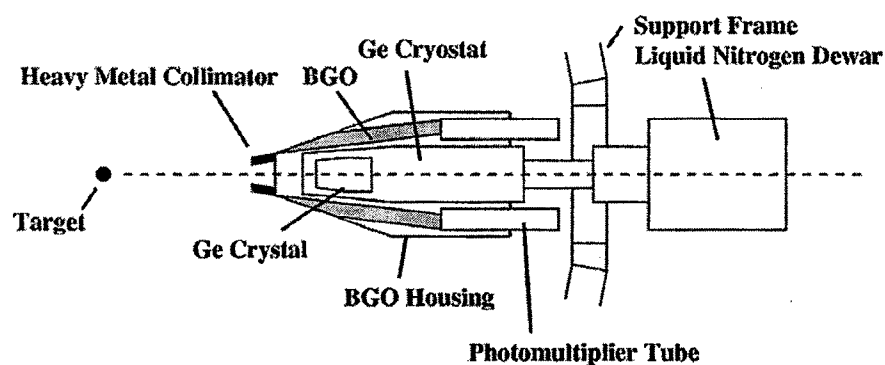


Figure 3.13: A Ge detector with tapered rectangular cryostat, cylindrical liquid nitrogen dewar (LN_2) and covered with a BGO shield.

3.9. Resolving Power of an Array

In a fusion-evaporation reaction, a large number of nuclei are populated leading to a complex spectrum with overlapping peaks. Gating by a specific transition in a nucleus (or by channel selection using auxiliary detectors) would select all the γ -transitions in a specific nucleus. Selecting a few of the transitions in coincidence would allow us to identify the levels in a specific band. Weak transitions in a band that are buried under the overlapping peaks in the singles spectrum can often be enhanced by appropriate selection of the gating condition.

The *resolving power* of a detector array is defined as its ability to identify weak peaks above the continuum background.

3.10. Data Acquisition and Analysis of Data from Multi-Detector Arrays

In an experimental setup containing a large number of detectors, a dedicated Data Acquisition System (DAS) is required to process the signals from the detector array. The primary objective of the DAS would be threefold:

- Process the analogue signals to obtain energy and timing information
- Decide which events need further processing using a hardware-based selection criteria (i.e. at least N number of detectors should have signals in time coincidence)
- Digitize the signals and save them in mass storage for further processing.

For the present generation of very large gamma rays (GAMMASPHERE, EUROGRAM, EXOGRAM, INGA, AFRODITE), typical requirements are

- Data rates upto 104 per event
- Collection of more than 200 parameters per event
- Storage of more than 1012 bytes of data per experiment.

The need to provide a large number of data channels in a typical experiment puts severe constraints on the design of the front-end electronics. Some of the basic characteristics of the instrumentation are:

- Increased reliability of operation
- High degree of integration to minimise the space and power requirement and reduction of inter-collecting cables.
- Replacement of manual controls by software control.
- Provision of remote monitoring of data

- Faster data handling to support the large event rate and increase number of parameters per event
- Modular development to allow integration with data from auxiliary detectors.

3.11. INGA Array

INGA: Indian National Gamma Array

The measurement of the coincidence between two γ -rays produced in a nuclear reaction plays a very important role in the assignment of the observed levels in the decay scheme, which help us in understanding the level structure at high spins. However, for in-beam measurements, the summing effects and Doppler broadening constrain the solid angle subtended by individual detectors to less than 0.5%. This considerably reduces the coincidence counting rate between two detectors. This results in lack of statistics to explore the high-spin states that are weakly populated.

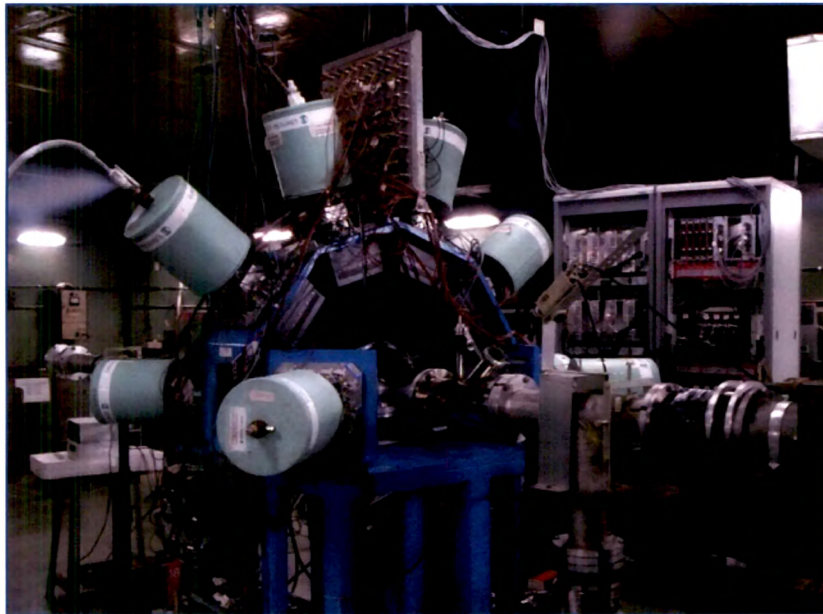


Figure 3.14: A photograph of Indian National Gamma Array (INGA) with 8 Compton suppressed Clover detectors at Variable Energy Cyclotron Centre (VECC).

One way of increasing the coincidence rate without compromising on the individual detector performance is to use a multi detector array *i.e.* an array of Compton suppressed Ge detectors. For N detectors, the two-fold coincidence rate between any pair

of detectors is increased by a factor of $N \times (N-1)/2$ in comparison to a 2 detector system. As mentioned earlier, a Clover detector has unique advantage over single crystal detector. Hence, a multi-Clover array will be beneficial to explore the phenomenon occurring at high spin due to the enhanced efficiency of a Clover detector.

Attempts to pool up the available resources to setup a multi Clover array were initiated by UGC-DAE Consortium for Scientific Research, Kolkata Centre (UGC-DAE, CSR) (formerly Inter University Consortium for DAE Facilities, IUC-DAEF). The first Clover array was setup at Tata Institute of Fundamental Research (TIFR), Mumbai, jointly by UGC-DAE-CSR, TIFR and Andhra University, Waltair. It consisted of 5 Clover detectors. The success of this experiment paved way for a national collaboration between UGC-DAE-CSR, Kolkata Centre, TIFR Mumbai, Saha Institute of Nuclear Physics (SINP) Kolkata, Variable Energy Cyclotron Centre (VECC) Kolkata, Inter University Accelerator Centre (IUAC) (Formerly Nuclear Science Centre – NSC) New Delhi and several Universities to setup an eight Clover array at TIFR Mumbai. Based on the success of these two campaigns at TIFR Mumbai, it was decided to reassemble the array at IUAC, New Delhi in 2002. After the successful zero, first phases of INGA at TIFR, Mumbai and second phase at IUAC, New Delhi, the INGA in the third phase of its instigation was brought to VECC, Kolkata. The first part of the experimental investigations presented in this thesis work were carried out using the 6 and 8 Clover array then stationed at VECC, Kolkata. In the experimental setup the Clover detectors were placed in 2 rings at 40° , 90° and 125° with respect to the beam direction. A total of 6 Clover detectors for the first experiment ($^{20}\text{Ne} + ^{27}\text{Al}$) were employed with 2 detectors at each on the angles. And for the second experiment ($^{20}\text{Ne} + ^{51}\text{V}$) 8 Clover detectors were used with 2 each at 40° , 125° and 4 at 90° with respect to the beam direction. The photograph of INGA at VECC is shown in Fig. 3.14.

3.11.1. Electronics for the Indian National Gamma Array (INGA)

The electronics for the γ -ray detector array is basically aimed at achieving the following:

1. To extract the energy and timing information from the pre-amplifier signals of the detectors.
2. To reject the events associated with the Compton scattering.
3. To generate a master gate, this indicates that the event under process is a valid event and can be recorded. In a typical γ - γ coincidence experiment, the master gate is

generated when two or more Compton suppressed γ -rays are in coincidence within the stipulated time window.

4. Digitizing and recording the information from all the detectors that have data for a valid event.

Channel selective 'exclusive' data collection has been possible due to the parallel developments: (i) better detectors having lower cost (ii) good energy per channel (iii) increase of speed in computation; has allowed the analysis of large volume of data.

The front end electronics of the INGA at VECC has provided us:

- 8 Energy signals from 8 Clover detectors
- 8 timing signals
- Anti-Compton logic for each Clover
- Coincidence logic for Compton-suppressed γ - γ and γ - γ - γ fold.
- Multiplicity logic for unsuppressed gamma fold
- Gating and pile up rejection for individual channels
- Electronics for auxiliary detectors like LEPS, recoil separator, charged particle array, neutron array etc.
- Synchronization logic to ensure parallel readout from multiple crates

Timing signals are derived for each of the four segments of a Clover detector. A delayed logic signal is provided for Compton-suppression of the individual segments. The total number of modules used in INGA array is large to fit within a single CAMAC crate. A scalable Multi-crate data acquisition system has been developed for distributed parallel readout and analysis data. Linux Amplified Multi-Parameter System (LAMPS) [14] software is used for data acquisition. List mode data contains event by event energy and timing information from all detectors. Online monitoring of singles projection and γ - γ matrix is provided.

3.11.1.1. Electronics for Compton Suppression

The block diagram of the electronics used for the experiment performed with INGA setup is shown in Fig. 3.15. The timing signal from a Clover detector is obtained from a combination of Timing Filter Amplifier (TFA) and a Constant Fraction Discrimination (CFD).

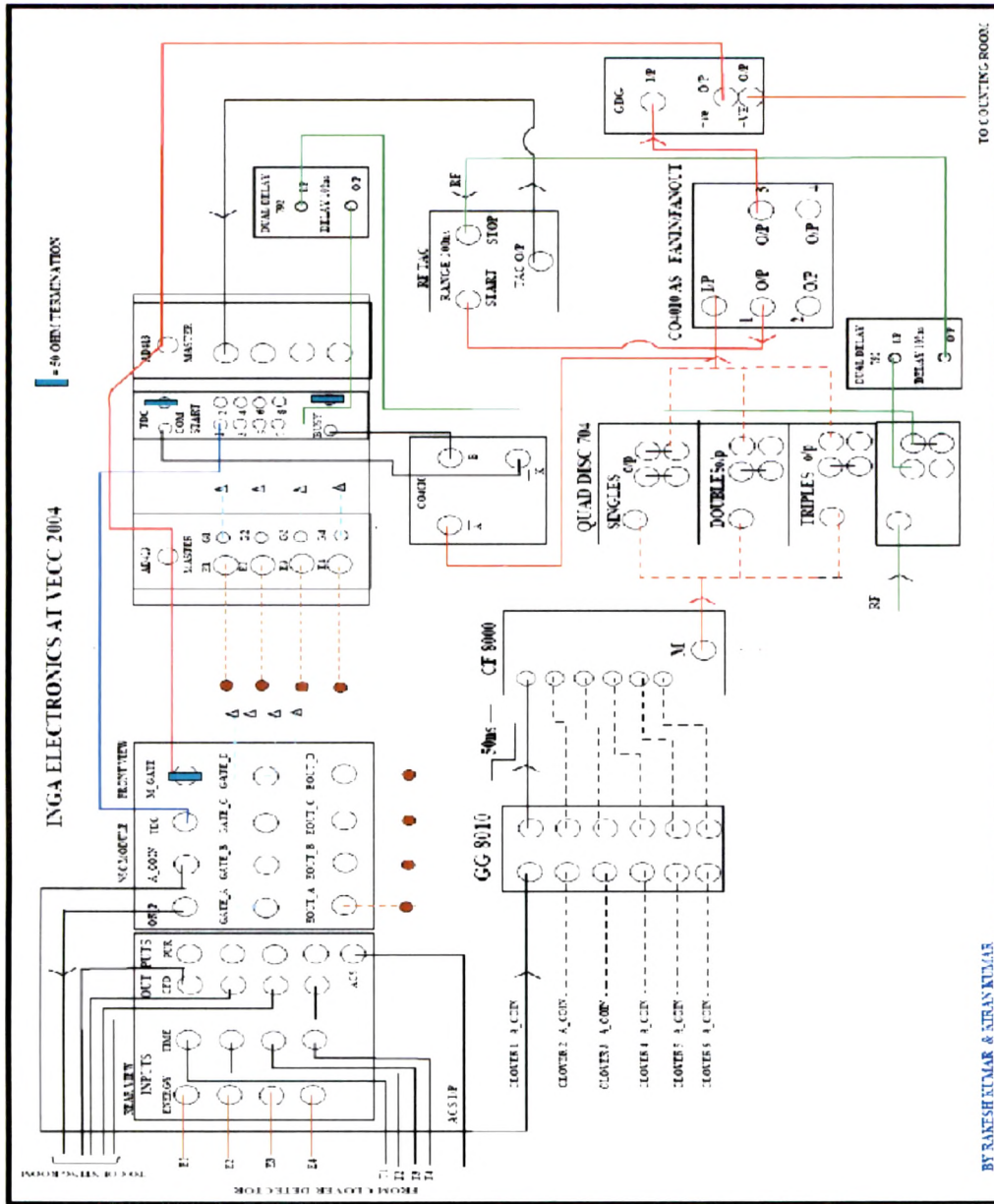


Figure 3.15: Schematic of the INGA (with 6 Clover detectors) electronics at VECC, Kolkata.

The threshold setting for the CFD is of a paramount importance. The threshold should be set low enough to record low energy events, but is sufficiently above the noise level. The timing signal from the BGO shield is also processed via a TFA-CFD combination. The BGO CFD threshold is adjusted around 30 keV in order to ensure that the low energy Compton scattered γ -rays are efficiently detected. Since the BGO has a

better timing response than the Clover detector, the BGO signal is made about 300 ns wide, with the Clover pulse being delayed by about 50 - 100 ns, to make it coincide with the centre of the BGO timing pulse. This ensures a better performance from these signals in the subsequent logic unit. These two signals are now used as inputs to a logic unit, CO 4010 for obtaining a $\overline{\text{Ge.ACS}}$ (Anti-Compton Shield) signal. The CO 4010 unit has both NIM and TTL outputs; the NIM signal is fed to the trigger logic unit to generate the Master Gate, while the TTL output is used to gate the ADC.

3.11.1.2. Generation of the Master Gate (Trigger Logic)

The basic circuit for the generation of the Master Gate is shown in Fig. 3.15. the $\overline{\text{Ge.ACS}}$ is fed to a majority coincidence unit, which provides a Sum/Multiplicity output that is proportional to the number of non-zero inputs. For example, the output is typically 50 mV per non-zero input. Hence a single-fold event results in a 50 mV output pulse, while a two-fold event results in a 100 mV pulse and so on (see Fig. 3.16). The signal is then connected to a discriminator, whose threshold can be set to accept the desired coincidence fold.

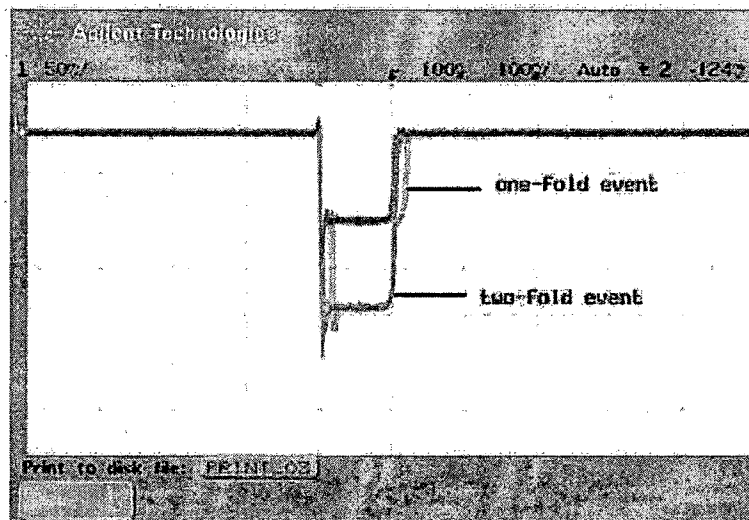


Figure 3.16: Figure shows the single- and double-fold output from a discriminator.

The final Master Gate is then generated from the signals from the Data Acquisition, such as the $\overline{\text{BUSY}}$. The Master Gate is then ANDed with the individual

$\overline{\text{Ge.ACS}}$ signals and stretched appropriately before being used to gate the individual energy signals from the Clover detectors.

3.11.1.3. Data Collection

The data recorded during the in-beam experiments could be classified as:

a. Singles Data

These correspond to the energy information from various detectors. The data is usually uncorrelated *i.e.* the data is recorded without sorting the data flow or the history of events. The data is recorded as multi-channel histograms, where the channel number is proportional to the pulse height. And counts/channel refers to the number of times a pulse height is observed within a fixed recording time interval.

b. List Mode Data

It consists of a sequence of correlated events and corresponds to energy and timing information from a group of detectors in coincidence. An event represents the set of numerical values associated with a physical event, where the recorded parameters are correlated in time, and to preserve this correlation, they are recorded in an event-by-event mode onto a storage device. The subsequent analysis of this data is discussed in detail in the next chapter.

3.12: AFRODITE Array

AFRODITE: AFRican Omnipurpose Detector for Innovative Techniques and Experiments [15]

AFRODITE array the iThemba LABS, South Africa, comprised of two sets of High Purity Germanium (HPGe) detectors, the Low Energy Photon Spectrometers (LEPS) and Clovers. AFRODITE in its present configuration, (Fig. 3.17), was commissioned in January 1998. It is a medium sized array that has the unique capability of detecting both high and low energy photons with a reasonably high efficiency by combining large volume escape suppressed HPGe detectors (Clovers) with Low Energy Photon Spectrometer (LEPS) detectors [15]. It has an aluminum frame with a rhombicuboctahedron shape with 16 detector positions. The detectors are positioned in 3 rings with angles at 45° (4 positions), 90° (8 positions) and 135° (4 positions) relative to

the beam direction (as shown in Fig. 3.18). The AFRODITE comprises of 8 Clover detectors and 8 LEPS for photons with energies between 30 and 300 keV.

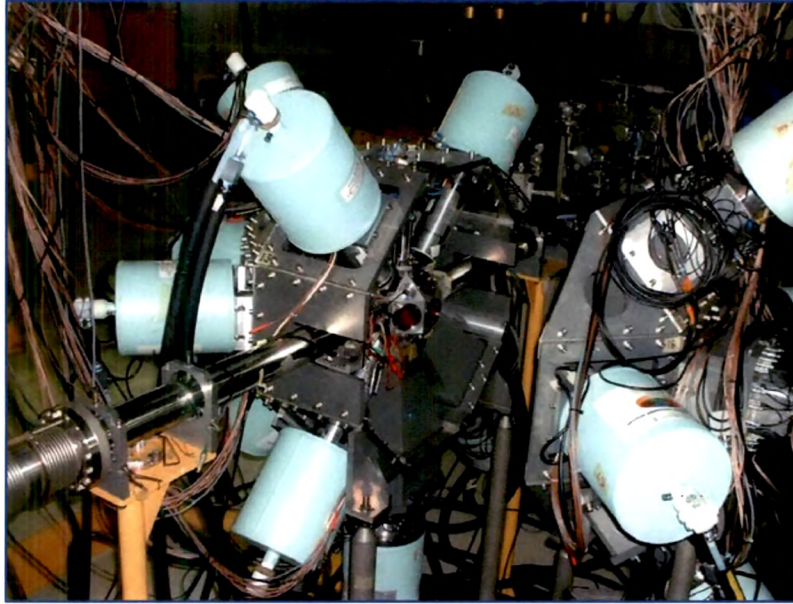


Figure 3.17: A photograph of the AFRODITE array consisting of 8 Compton suppressed Clover detectors and 4 LEPS detectors at iThemba LABS.

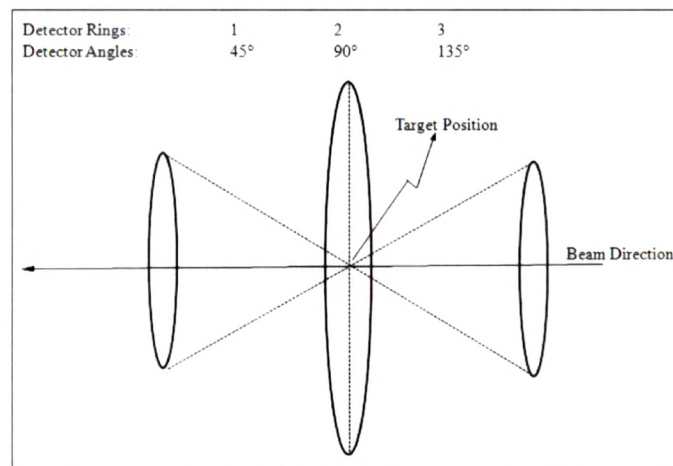


Figure 3.18: Schematic representation of the three detector rings of the AFRODITE array.

The eight Clover detectors used subtend 11% of 4π and have a total photopeak efficiency of 2% at 1.33 MeV. The LEPS consist of four segmented planar Ge detectors of $2800 \text{ mm}^2 \times 10 \text{ mm}$ and they subtend 12.5% of 4π . The Clover detectors are each

housed in a Compton suppression shield that is made of bismuth germanate (BGO), which is a highly efficient scintillator for the detection of γ - rays.

It is worth mentioning that this configuration allows significant shielding of the detectors from radiation emanating from the scattering beam. The aluminium frame supporting the 15 germanium detectors may be retracted from the beam line to allow access to the target chamber, as shown in Fig. 3.19.

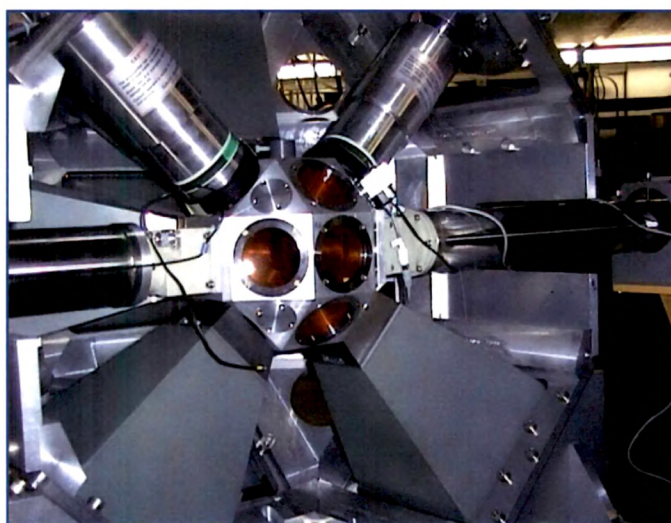


Figure 3.19: AFRODITE array and the target chamber with its kapton windows. A camera is mounted on the top right – hand triangular facet.

3.12.1. An Overview of the Electronics used

The CAMAC and NIM Electronics fall into three broad categories: (i) *linear electronics* that maintain a linear relationship to the size of the initial signal, (ii) *logic circuits* that provide only a standard (or single sized) pulse indicating that a given logical condition was met, and (iii) *data – acquisition* for recording the data [16].

The NIM and CAMAC electronic units were connected according to the circuit diagram depicted in Fig. 3.20. Standard NIM and CAMAC modules located in the experimental vault perform signal processing. Data acquisition used for this experiment was based on the MIDAS software package and the whole data acquisition system is directed from the data room. The MIDAS software was employed before (for energy calibration) and during the experiment. It was also used to monitor online spectra, event rate and data acquisition in general. Some of the adjustable parameters (e.g. amplifier

gains, shaping times and pole zero settings for the LEPS) can be set from the data room although trouble shooting the electronics is only possible from within the vault itself. To explain the electronics used in this experiments let's look at the simple electronic circuit as shown in Fig. 3.20.

The electronic diagram depicted in Fig. 3.20. consists of two sub - circuits, namely, (i) a timing circuit, which is used to time-correlate the detected γ - rays and (ii) an energy circuit, which gives us information about the energy of the detected γ - rays. This energy information will then be used in the construction of γ - γ matrix.

3.12.1.1. Energy Circuit

In most cases the detected energy is related to the total charge produced in the detector. For the best achievable energy resolution an optimum filter has to be implemented which takes into account the response as well as the noise characteristics of the instrument. The essential element for signal processing chain is the pre- amplifier housed in the detector cryostat and is usually located as close as possible to the detector in order to minimize the noise signal [17]. In earlier detector systems, cables were used to connect the detector to the pre-amplifier, but presently the pre - amplifier comes as an integral part of the detector assembly. This implies that the pre-amplifier is cooled down whenever the detector system is being cooled, which also reduces the electronic noise. The pre - amplifier in general can have various modes of operation: current - sensitive, voltage - sensitive and charge - sensitive. The main purpose of the pre- amplifier is to match the impedance of the detector (which is a measure of the opposition to the flow of an alternating current). The charges are created within the detector by the interaction with the gamma-radiation and are then collected by the pre - amplifier, which converts the charge pulse to a voltage pulse and drives the pulse to the next element in the circuit, which is the spectroscopy amplifier [18].

The pre-amplifier output pulse is ≈ 100 mV with a decay time of 50 μ sec and is fed to the spectroscopy amplifier. The amplifier gives two outputs, which are the fast and the slow output. The fast output is used for the timing circuit and the slow (energy signal) output is used for the energy circuit. For the slow signal the essential function of the amplifier is to amplify the signal from the pre-amplifier and shape it into a Gaussian pulse, so that the pulse height can be measured.

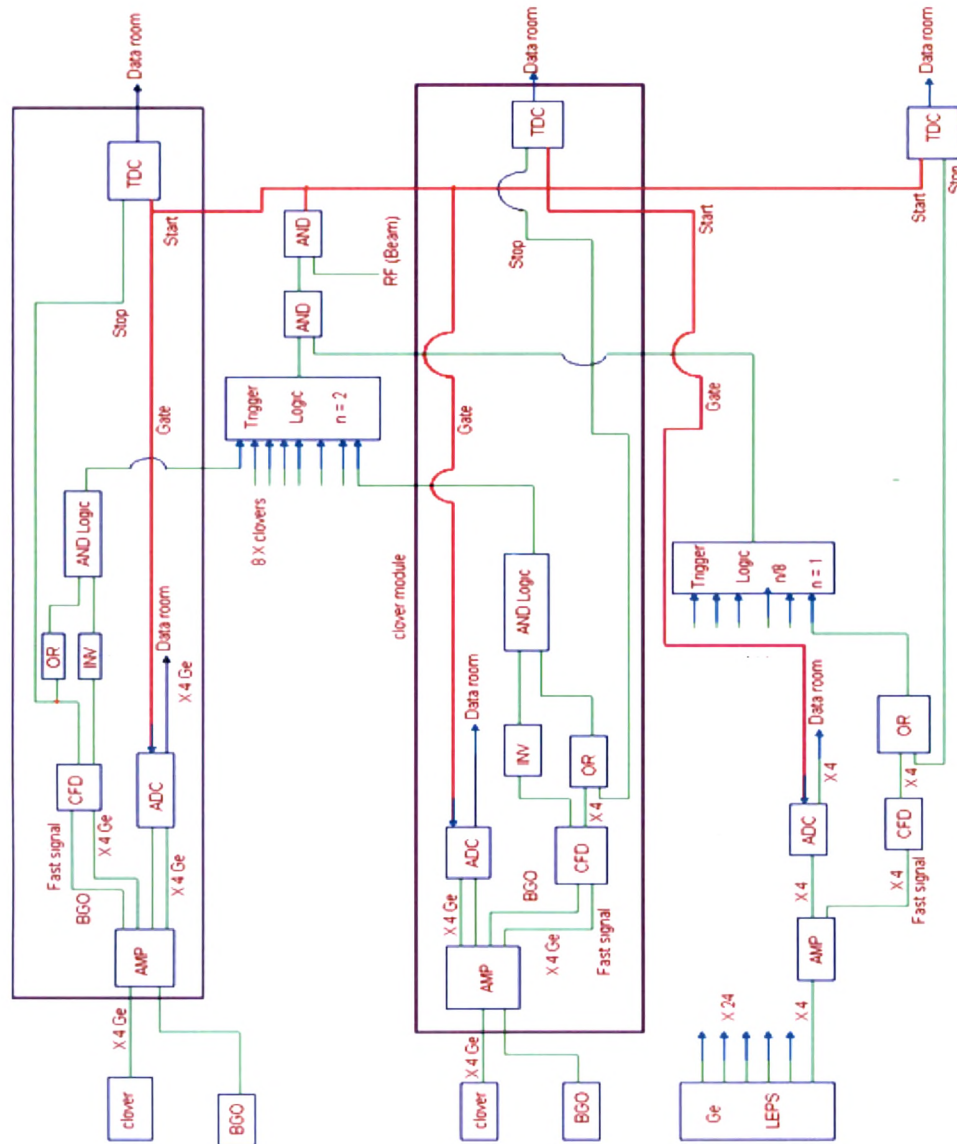


Figure 3.20: The AFRODITE array electronics setup for the experiment.

This is done by electronically differentiating and integrating the input signal and gives an output linear pulse, whose height is proportional to the γ - energy. The other setting of the amplifier, called the pole zero cancellation differentiation, removes the overshooting and undershooting of the signal and allows the system to work under moderate count rate without loss of resolution. (This was done in the vault during the experiment setup). The slow energy signal is fed to the ADC (Analog - to - Digital Converter).

3.12.1.2. Timing Circuit

To determine the time of the incoming particle (e.g. the start of the signal) FIR (Finite impulse response) filters or procedures are used in analog circuit, such as the constant – fraction method. The timing circuit establishes all the coincidence relationships between signals from different hardware components for a specific experiment. Here a signal from the BGO was used to veto the corresponding Clover signal and coincidence was set between at least two “clean Ge” signals.

The pre-amplifier produces a negative shape pulse that goes to an amplifier (CAEN), which gives out a narrow negative signal. The output signals (from BGO and Ge) are fed to the CFD (Constant Fraction Discriminator) where they are converted to logic signals, which are required by the timing circuit. The BGO logic signal from CFD is inverted and fed to AND logic module to check the coincidence between the BGO and Clover. The condition for coincidence is met when both input signals are present in the AND logic. If any one of the signals is not present the AND logic module will give zero output. Thus the AND module is going to give an output logic signal provided the BGO is not hit by a gamma ray.

The four Clover element logic signals are sent to an OR module, which gives an output provided at least one signal is present. The output signal is then fed to the trigger logic, where the module will determine whether there is a coincidence between the Clovers. The trigger logic gives an output if there is a coincidence between at least $n_1 = 2$ Clover signals. This logic signal is sent to another AND logic to check whether there is also a coincidence with at least $n_2 = 1$ LEPS detectors. Finally the signal is connected to another AND logic module for checking the coincidence with the beam RF logic signal. The output signal is fed to the ADC (as ADC gate signal) and to the TDC (as common start signal) modules. The TDC (time to digital converter) in the CAMAC crate has two inputs, which are common start and stop. Here the TDC produces digitalized output corresponding to the time between the start and stop signals. The TDC stop signal is provided by the first fast detector signal to arrive at the TDC after the TDC start pulse. Individual detectors generate the stop pulses. The digitized TDC output signal is sent to the data room.

References:

1. A. Johnson, H. Ryde, J. Sxatarkier, Phys. Lett. 34B, 605 (1971)
2. R.M. Leider, H. Ryde, Advances in Nuclear Physics 10, 1 (1978)
3. P. Twin *et al.*, Phys. Rev. Lett. 57, 811 (1986)
4. K.S. Krane, "Introductory Nuclear Physics" (Wiley, 1988)
5. F.A. Beck, Prog. Part. Nucl. Phys. 28, 443 (1992)
6. C.W. Beausang, J. Simpson, J. Phys. G: Nucl. Part. Phys. 22, 527 (1996)
7. R.M. Leider, "Experimental Techniques in Nuclear Physics" (Walter de Gruyter, Berlin) 137, (1995)
8. P.J. Nolan *et al.*, Ann. Rev. Nucl. Part. Sci. 45, 561 (1994)
9. J. Gerl, R.M. Leider, GSI Dramstadt, Report (1992)
10. P.M. Jones *et al.*, Nucl. Instrum. Methods Phys. Res. A 399, 51 (1997)
11. G.F. Knoll, "Radiation Detection and Measurement" 2nd Edition, (John Wylie and Sons) New York, (1989)
12. I.Y. Lee, "Proc. In Exotic Nuclear Spectroscopy", ed. W.C. McHarris (Plenum press), 345 (1989)
13. P.J. Nolan *et al.*, Nucl. Phys. A 409, 343 (1983)
14. A. Chatterjee *et al.*, <http://www.tifr.res.in/~pell/lamps.html>
15. R.T. Newman, *et al.*, Proc. Balkan School on Nuclear Physics, Balkan Physics Letters, 182 (1998)
16. G.K. Mabala, Ph.D. Thesis, University of Cape Town (March 2000)
17. Gordon Gilmore, John D. Hemingway, "Practical Gamma-ray Spectrometry", 199-202 (1995)
18. William R. Leo, "Techniques for Nuclear and Particle Physics Experiments", 242-269, (1987)